High Performance SWIR Imaging Cameras

Raptor Photonics
Geoff Martin

Introduction to SWIR Imaging

Silicon based area detectors (e.g. CCDs or CMOS) are widely used in high performance imaging applications, detecting wavelengths from soft x-ray through to near infrared (NIR). Typically, the quantum efficiency (QE) of these detectors decreases rapidly as the detection wavelength increases further into the NIR region. Above 1100nm, Silicon is transparent and therefore cannot be used to directly detect photons of these wavelengths, however many other materials do have photon sensitivity at wavelengths of 1µm and longer. The definition for each 'sub-region' within VIS-IR wavelength range is outlined in Figure 1, along with some commonly used detector materials and their typical detection ranges. Each of the materials highlighted below present their own advantages and challenges and therefore prior to detector selection, the user must consider all aspects of the intended application, in addition to the wavelength response.

Many everyday objects appear markedly different when viewed in different wavelength bands, as illustrated in Figure 2, showing images of a bank note recorded at two different wavelengths. The image recorded at 550nm shows the printed images we see with our eyes, which enable us to determine that the object is a banknote as well as additional details such as the monetary value, the name of the bank which produced it and the location depicted on it. In the 1600nm image there are many different attributes clearly visible, including the creases in the note itself and some features from the other side of the note, such as the serial number, near the bottom left corner, and a foil emblem just above it. However, in the absence of the more familiar visible wavelength features we might struggle to determine exactly what object was being displayed, if presented with this SWIR-only image alone. This very basic example highlights the power of SWIR imaging to uncover additional features of an object, but also illustrates how important a sensor which responds also to visible light can be for providing context to images in certain applications.

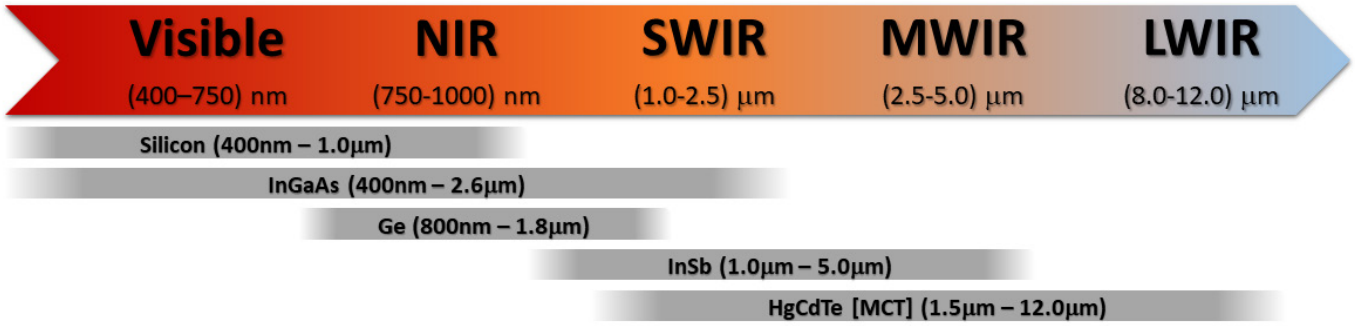

Figure 1: The various sub-regions of the electromagnetic spectrum, covering visible through to infrared wavelengths. Some common detector materials and their useful wavelength detection ranges are also listed.

Figure 2: Images of a bank note at two different wavelength bands. The left image was acquired at wavelength of (550 ± 10) nm whereas the right image is the same scene viewed at (1600 ± 12) nm.

The use of imaging systems to capture long wavelength photons (beyond the detection range of Silicon based devices) continues to increase in many diverse application areas, such as life sciences, security & surveillance, non-destructive testing, agriculture,environmental, quality control and astronomy.

This paper will be restricted to a discussion of the performance of InGaAs detector arrays, sensitive in the VIS-SWIR region, i.e. (550 – 1700) nm.

Brief Overview of InGaAs Detector Arrays

Detector Construction

InGaAs is a semiconductor material which is an alloy of Indium Arsenide (InAs) and Gallium Arsenide (GaAs). Detector arrays are produced by growing an epitaxial layer of InGaAs on an Indium Phosphide (InP) substrate, with a thin passivation layer of InP grown on top of the InGaAs. The doped substrate and InGaAs layer are used to construct a photodiode array (PDA) which delivers photosensitivity, typically for wavelengths between (900 – 1700) nm. The individual pixels of the photodiode array are then bonded to a CMOS ROIC (ReadOut Integrated Circuit), see Figure 3, which is used to perform the charge to voltage conversion, A/D conversion and transfer of data from the sensor. Historically Indium bump bonds were used to attach the imaging array to the CMOS ROIC, which imposed some practical limitations on both the physical size and the pixel pitch of commercially available devices.

This hybrid sensor fabrication results in the PDA being illuminated through the substrate layer, as illustrated in Figure 3. Absorption in the (relatively) thick InP substrate layer prevents photons with wavelengths below ≂900nm reaching the PDA, explaining why many InGaAs sensors have poor response to wavelengths below this value.

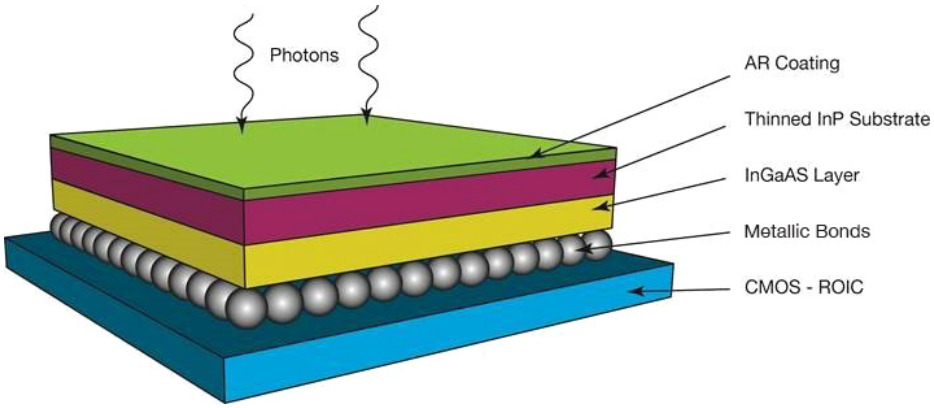

Figure 3: Schematic representation of the main components used in the construction of a VIS-SWIR InGaAs detector array.

However, the sensors used in the NINOX camera have the bulk of this substrate layer removed (i.e. thinned away), producing a detector with response across visible, NIR and SWIR regions. A broadband AR coating is also applied to the thinned PDA, producing a detector array which has excellent QE across the SWIR and NIR regions and good QE extending into the visible region, see Figure 4. These VIS-SWIR detectors can provide

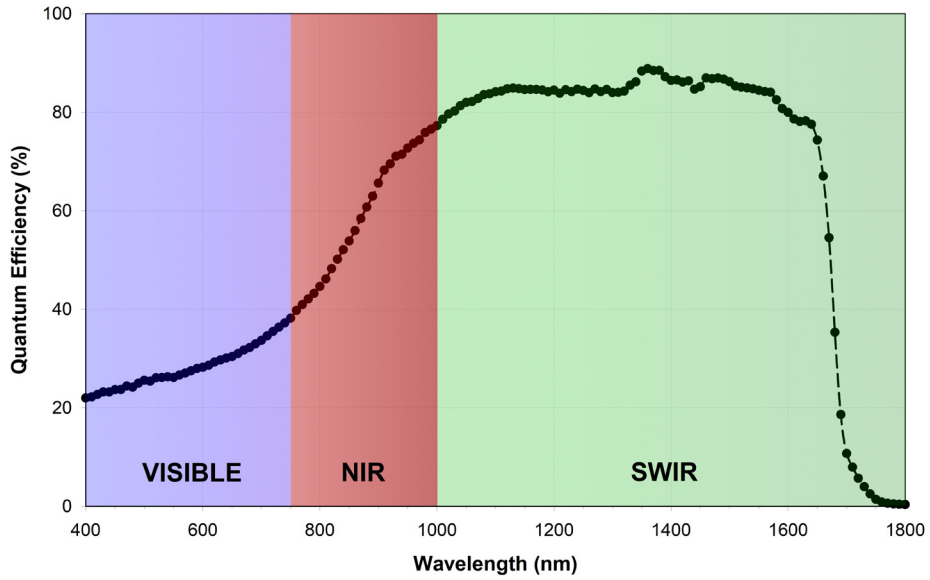

Figure 4: Typical QE curve for a thinned, AR-coated, VIS-SWIR InGaAs detector array, as used in the Ninox camera.

high performance imaging capability, enabling the user to observe objects at all wavelengths between approximately 550nm in the visible region and 1700nm in the SWIR regions, using a single camera.

The cut-off at long wavelengths is determined by the bandgap of the InGaAs material from which the sensor is constructed. Unstrained In0.53Ga0.47As is lattice matched to the InP substrate and has a bandgap of approximately 0.75eV at room temperature, corresponding to a cut-off wavelength just below 1700nm. Increasing the fraction of InAs within the alloy reduces the bandgap, shifting the cut-off to longer wavelengths. The material is no longer lattice matched to the substrate and this 'strained' or 'extended' InGaAs has been used for detection up to ≈2.6µm. However, this extended response does come with some penalties, in particular, higher dark current, more defects per device and increased cost.

The bandgap of the InGaAs material is also temperature dependent and increases as the sensor temperature is decreased. As a result, cooling the device causes the long wavelength cut-off in the response curve to move to shorter wavelengths.

All the data presented within this paper was acquired using lattice matched, thinned InGaAs sensors providing VIS-SWIR response as indicated by the QE plot in Figure 4.

Detector Properties and Performance

The inherent complexity of manufacturing this type of imaging device has limited the pixel sizes available to relatively large dimensions, historically ≥10µm and can result in both low manufacturing yields and the presence of defective / non-operational pixels within the final device. However high-quality devices, such as those used in the OWL and NINOX range of cameras, have pixel operability >99.5% due to years of process optimization for device manufacture.

Available array sizes are small, when compared to CCDs / CMOS imaging devices, the largest, widely available array size is currently 1280 x 1024 pixels.

A small number of InGaAs devices with 5µm pixels are just starting to enter the market, primarily in VGA format (in addition to one SXGA offering). Manufacture of some of these devices has implemented Cu-Cu bonding1 (instead of Indium bump bonds) for attaching the FPA to the CMOS ROIC. Future generations of these devices could (theoretically) decrease the pixel size further and / or yield larger array sizes, potentially unlocking new applications and market segments for InGaAs image sensors.

The unit cost of high performance InGaAs FPAs is significantly greater than a Si-based detector of the

[1] S. Manda et al., "High-definition Visible-SWIR InGaAs Image Sensor using Cu-Cu Bonding of III-V to Silicon Wafer.," 2019 IEEE International Electron Devices Meeting (IEDM), San Francisco, CA, USA, 2019, pp. 16.7.1-16.7.4, doi: 10.1109/IEDM19573.2019.8993432.

same array size, primarily due to the intricacies involved with the handling and manufacturing of the component pieces and final assemblies.

The use of a high performance CMOS ROIC delivers some advantages and disadvantages, analogous to those found on conventional Si CMOS imagers, e.g. high frame rates are achievable, short exposure times down to 1µs can be realized and global shutter (snapshot) operation is implemented on the sensor used within the NINOX camera range. However Non-Uniformity Corrections (NUCs) must be applied to reduce fixed pattern noise (FPN) introduced by the CMOS ROIC. The NUC on the NINOX camera can be switched ON / OFF within the control software.

In addition to the increased sensor costs and FPN, the two main disadvantages associated with InGaAs detector arrays have been high readout noise and high dark current.

Readout Noise

The readout noise is strongly influenced by the quality / performance of the CMOS ROIC integrated within the detector. Historically ROIC designs provided typical readout noise levels in the range 200 – 700 electrons, depending upon the amount of gain applied. This is acceptable for use in thermal imagers and the detection of 'bright' signals, provided there is sufficient pixel well depth to store signals large enough to overcome the high noise floor and provide an acceptable signal to noise ratio.

However low light detection was not possible with these ROICs and the intra-scene dynamic range was limited. The latest generation of ROIC design has been utilized in the NINOX 640 II camera and enables data to be readout via one of two gain modes:

i. High Gain (HG) Mode – offering the lowest readout noise (≈18e-) with limited pixel well depth (>10ke- pixel)

ii. Low Gain (LG) Mode – for maximum dynamic range, offering the maximum pixel well depth (>200ke- per pixel) but with increased readout noise (≈150e-). This provides an intra-scene dynamic range >62dB.

Dark Current

The small bandgap of InGaAs (≈0.75eV at room temperature) means that it is much easier to thermally promote electrons from the valance band into the conduction band, compared to silicon for example. This manifests as a significantly higher dark current in InGaAs detectors, when compared to silicon-based detectors with similar pixel sizes. Some early generation devices suffered from dark currents of the order 106e-/pix/sec (≈160fA/pix) at room temperature (+25°C), approximately four orders of magnitude higher than pinned silicon-based detectors. Obviously, this level of dark current severely limits the range of exposure times that could be used for image acquisition, as dark signal and its associated shot noise rapidly became the dominant features in acquired images. Detector manufacture has improved, reducing dark current to the order of ≈104e-/pix/sec (≈1.6fA/pix) at room temperature.

The NINOX camera utilizes Raptor Photonics PentaVac™ technology and actively cools the InGaAs FPA to reduce the dark current to approximately 250e-/pix/sec (approx. 0.04fA/pix). This is achieved using only moderate cooling power, attaining a detector temperature of approx. -30°C, thus minimizing the shift in the long wavelength response cut-off and maintaining a compact camera form factor.

Inferior ROIC architectures and designs can necessitate much deeper cooling of the sensor, e.g. to -80°C or lower, in order to achieve comparable dark current performance. These cryogenic / deep-cooled camera systems are typically physically much larger in size, significantly more expensive and result in much larger shifts in the long wavelength response cut-off.

The final camera performance is determined by a combination of the quality of the InGaAs PDA and the performance of the CMOS ROIC, in addition to the design and implementation of the camera electronics and firmware. The NINOX camera has optimized all these components to deliver the best scientific performance available from a VIS-SWIR imaging camera, as detailed in the following sections.

Dark Current (and Dark Noise) Reduction

Cooling the InGaAs FPA provides a dramatic decrease in the measured dark current per pixel, as shown in Figure 5 below. The calculated dark current doubling temperature is approximately 7°C, which is similar to the dark current temperature dependence observed on Silicon based FPAs.

The NINOX camera employs thermoelectric cooling inside a PentaVac™ vacuum enclosure to provide a compact and maintenance-free method of cooling the sensor to temperatures of ≤-15°C. As can be seen from Figure 5, the cooling performance offered by the NINOX camera translates to a dark current reduction of two orders of magnitude, when compared

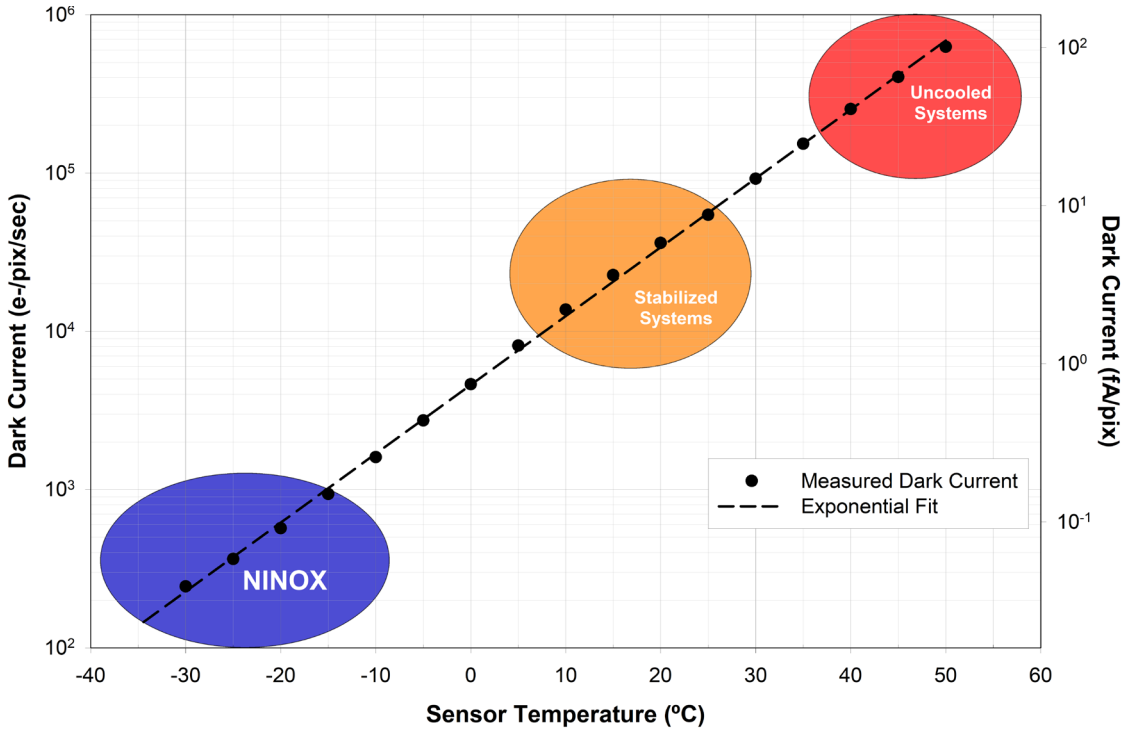

Figure 5: Typical variation of measured dark current with temperature for the InGaAs FPA used within the NINOX camera.

The diverse range of applications for which VIS-SWIR image detectors can be used place a variety of requirements on the camera / imaging system, including the use of different gain modes, frame rates and exposure times.

Some applications may require little or no cooling in order to deliver the required performance, however some more demanding applications may benefit from cooling the InGaAs FPA to temperatures 40°C or 50°C below the ambient, in order to reduce dark current shot noise and increase the accessible dynamic range.

Uncooled systems typically operate with sensor temperatures between +40°C to +50°C, whereas stabilized systems operate with a sensor temperature typically in the range +10°C to +25°C.

to a room temperature, stabilized system and more than three orders of magnitude, compared to an uncooled system operating at +50°C.

The effect of dark current on the image can be visualized by comparing dark frames of equal exposure time, acquired at different sensor temperatures, as shown in Figure 6. The higher dark current is clearly visible as speckle in the 2 second dark frame acquired at +30°C. Plotting a horizontal cross section (through the centre of the image) helps to visualize the impact the dark current and associated shot noise will have on any image acquired under these conditions. The presence of relatively high pixel values in this dark frame indicate that a significant fraction of the pixel full well capacity is being wasted, as it is storing dark signal as opposed to any signal the user is attempting to capture.

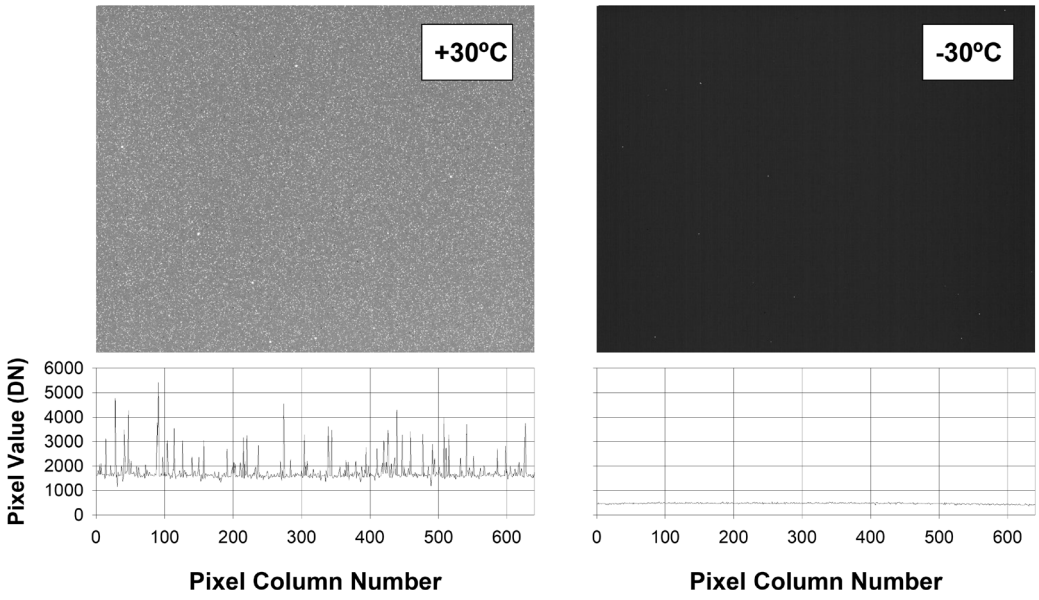

Figure 6: 2 second dark frames acquired at sensor temperatures of +30°C and -30°C. Note the same grayscale is used for both images. The line plots are horizontal cross sections along the central row of each image.

The spikey nature of the image, indicative of a raised noise, in this case due to dark current shot noise, will degrade the final image quality as any detected signal will be superimposed upon this noise floor. The combination of these two effects, reduced useable full well capacity and increased noise floor, will severely limit the maximum signal to noise ratio which can be achieved under these operating conditions. However assessing the 2 second image which was acquired at a sensor temperature of -30°C, it is evident that relatively little of the pixel well capacity has been consumed by dark current and also the noise floor is dramatically lower as a result of the reduction in dark current.

An alternative means of assessing the impact of cooling the sensor is to compare histograms of dark frames, for a device at two different test temperatures. Figure 7 compares histograms of 100ms exposures taken at sensor temperatures of +20°C and -20°C (in high gain mode). The impact of dark current is clearly visible as the peak pixel occurrence shifts to a higher value at the warmer sensor temperature. Not only does this dark current introduce a higher dark current shot noise component, but it also partially fills the wells of the pixels, which prevents this portion from being used to capture image data by the user. So, it is clear that these effects will be detrimental to both the signal to noise ratio and the accessible dynamic range of the detector system.

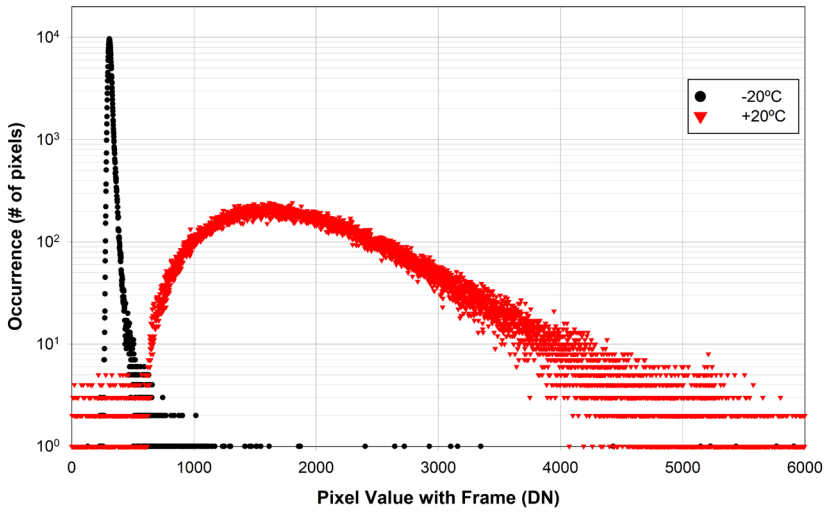

Figure 7: Histogram plots of 100ms dark frames taken at two different sensor temperatures in high gain mode.

Using typical values for sensor read noise and dark current, it is possible to estimate the theoretical 'accessible dynamic range', which we define as follows:

$$\text{Accessible Dynamic Range} = \frac{\text{Accessible Pixel Well Depth}}{\text{Dark Noise}}$$

$$= \frac{\text{Pixel Full Well Capacity} - \text{Dark Signal}}{(\text{Read Noise}^2 + \text{Dark Shot Noise}^2)^{1/2}}$$

$$= \frac{\text{Pixel Full Well Capacity} - \text{Dark Signal}}{(\text{Read Noise}^2 + \text{Dark Signal})^{1/2}}$$

$$= \frac{\text{Pixel Full Well Capacity} - (\text{Mean Dark Current} \times \text{Exposure Time})}{(\text{Read Noise}^2 + [\text{Mean Dark Current} \times \text{Exposure Time}])^{1/2}}$$

Producing a plot of this accessible dynamic range as a function of exposure time can indicate to the user the parameter space over which the camera will serve as a useful detector, delivering a specific dynamic range. Examples of these plots are shown in Figure 8, which show the typical operation of the NINOX 640 II camera, operating with a sensor temperature of -20°C compared to the same sensor operating at a temperature of +20°C.

The graph clearly shows the benefit of cooling the InGaAs FPA, as the accessible dynamic range for both gain modes are preserved for longer exposures, up to a few tens of seconds for the high gain mode and up to several hundred seconds for the low gain mode.

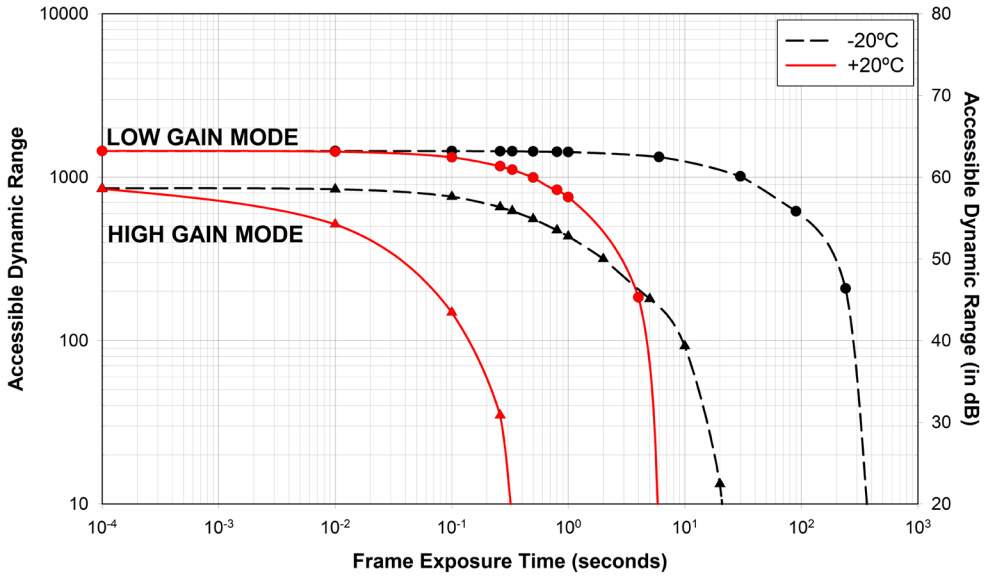

Figure 8: Plots of 'Accessible Dynamic Range' versus exposure time for the NINOX 640 InGaAs FPA at two different temperatures. Low gain mode maximizes dynamic range whereas high gain mode minimizes readout noise.

Photon Transfer Curve and Linearity

Constructing a photon transfer curve for the camera allows the user to quantify the performance of the camera. Variance photon transfer curves have been constructed for a NINOX 640 II camera at a sensor temperature of -15°C. Using the calculated conversion factors, the measured data can be converted from arbitrary units, i.e. Digital Numbers (or DN) into absolute units, i.e. electrons. Figure 9 shows a typical plot acquired on a NINOX 640 II camera, with the circular points showing the actual measured total noise as a function of mean signal level.

Further analysis of the data shows that the dark noise floor (due to readout noise and any dark current shot noise) is approximately 15 electrons in this configuration (high gain mode, sensor temperature = -15°C, exposure time 10ms) and the accessible full well capacity is approximately 12ke-/pixel in this gain mode. De-convolving the dark noise component from the total measured noise, should leave data which displays an ideal shot noise limited dependence, i.e. noise equal to the square root of the signal, indicated by the dashed line in Figure 9.

As can be seen from the graph there is excellent agreement between the theoretical line and the experimental data (triangular points) across the entire range of measured signal (approximately 20 – 12,000 electrons per pixel).

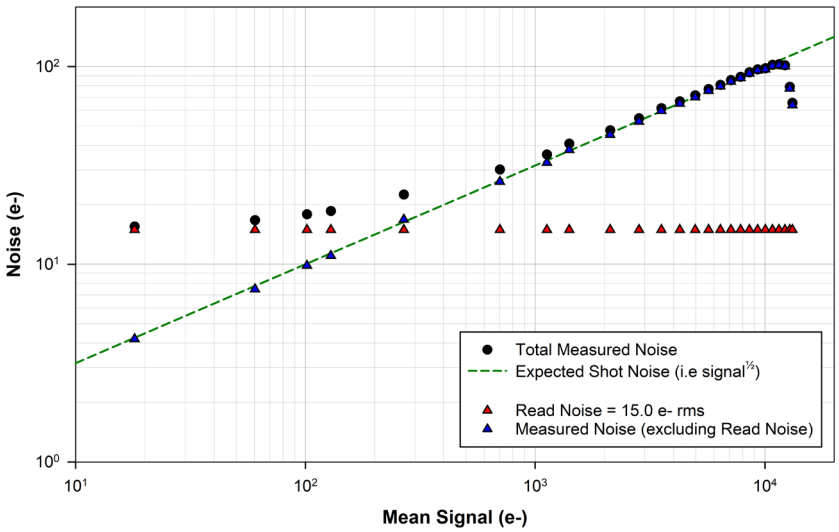

Figure 9: Sample Photon Transfer Plot for NINOX II camera, acquired in high gain mode with the sensor cooled to -15°C and an exposure time of 10ms. Excellent agreement between measured and theoretical shot noise performance across the entire range of measured signals.

The linearity performance of the NINOX 640 II camera is illustrated in Figure 10. This analysis also shows the expected agreement between measured data and a straight-line fit with a non-linearity of <0.4% calculated across the measured signal range.

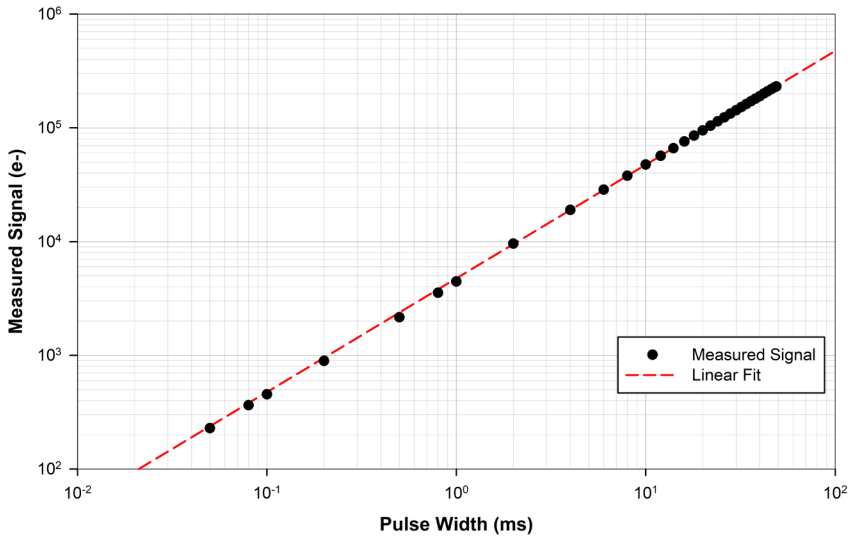

Figure 10: Linearity plot for NINOX II camera, acquired in high gain mode with the sensor cooled to -15°C and an exposure time of 10ms. Signal level was varied by changing the pulse width of the light source. Excellent agreement is observed between measured data and a straight-line fit, with the non-linearity being determined to be <0.4%.

Summary

Standard characterization techniques have been used to quantify the performance of a moderately cooled InGaAs FPA within the NINOX 640 II camera. The intra-scene dynamic range has been verified to be high (>60dB) with excellent linearity. Low noise performance is achieved through both high and low gain readout modes.

Cooling the FPA to a temperature ≤ -15°C significantly reduces the dark signal and associated noise within images, enabling acquisition of quantitative data with exposure times of up to several minutes. The improvement in image quality, as a result of this cooling, has been illustrated.

PentaVac™ technology enables moderate cooling of the InGaAs FPA using minimal input power. The shift in the long wavelength response cut-off is reduced, compared to cryogenically / deep-cooled systems, and therefore the NINOX camera range offers superior performance in an affordable, rugged, compact form factor.

Author Profile

Dr. Geoff Martin is a Physicist working at Raptor Photonics Ltd, based in Northern Ireland.

About Raptor

Raptor is a leading developer of high-performance digital cameras using CCD, EMCCD, CMOS and InGaAs detector arrays.

Raptor has spent many years developing both SWIR and VIS-SWIR technology into some of the highest performing cameras available today.

The selection of sensor type, required cooling performance and cooling method can be discussed with Raptor Photonics team to identify the ideal solution for your application.

For more information contact Raptor Photonics Ltd as follows:

sales@raptorphotonics.com or **Tel: +44 2828 270 141**

Raptor UK (Headquarters)
T: +44(0)2828 270 141
E: sales@raptorphotonics.com
www.raptorphotonics.com

Raptor USA
T: 1 (877) 240-4836
E: sales@raptorphotonics.com
www.raptorphotonics.com